

# Autonomy Architecture for Aerobot Exploration of Saturnian Moon Titan

Alberto Elfes, Jeffery L. Hall, Eric A. Kulczycki,  
Daniel S. Clouse, Arin C. Morfopoulos, James F. Montgomery,  
Jonathan M. Cameron, Adnan Ansar & Richard J. Machuzak  
*Jet Propulsion Laboratory*

## ABSTRACT

The Huygens probe arrived at Saturn's moon, Titan, January 14, 2005, unveiling a world that is radically different from any other in the solar system. The data obtained, complemented by continuing observations from the Cassini spacecraft, show methane lakes, river channels and drainage basins, sand dunes, cryovolcanos and sierras. This has led to an enormous scientific interest in a follow-up mission to Titan, using a robotic lighter-than-air vehicle (or aerobot). Aerobots have modest power requirements, can fly missions with extended durations, and have very long distance traverse capabilities. They can execute regional surveys, transport and deploy scientific instruments and in-situ laboratory facilities over vast distances, and also provide surface sampling at strategic science sites. This describes our progress in the development of the autonomy technologies that will be required for exploration of Titan. We provide an overview of the autonomy architecture and some of its key components. We also show results obtained from autonomous flight tests conducted in the Mojave Desert<sup>1,2</sup>.

## INTRODUCTION

In addition to Earth, seven other bodies in the solar system have enough of an atmosphere to allow aerial exploration:

Venus, Mars, Jupiter, Saturn, Uranus, Neptune, and Saturn's moon, Titan. The NASA 2003 Solar System Exploration Roadmap identified aerial vehicles as a strategic new technology for Solar System exploration [1], and emphasized the development of advanced autonomy technologies as a high priority area for the operation of aerial probes. NASA's 2006 Solar System Exploration Roadmap [2] confirms and extends this vision, listing future Titan and Venus in-situ missions using lighter-than-air vehicles (Figure 1) as two of its top three flagship mission priorities (the Titan Explorer and Venus Mobile Explorer missions, respectively). In-situ platforms are essential because of the dense clouds that cover Titan and Venus, limiting orbital surveys.

The dense atmospheres at Titan and Venus enable the use of buoyant robotic vehicles (aerobots) that can be either self-propelled (airships) or wind-driven (balloons). These vehicles can provide extensive, low-altitude geographical coverage over multi-month time scales with minimal consumption of scarce onboard electrical power [3-7]. Airships have the scientific advantage of being able to fly to specific locations, while balloons are simpler in their design, but limited in their "go-to" capability. Advantages and disadvantages of different aerial vehicle designs for planetary exploration are assessed in [8].

Herein, we focus on the challenges involved in aerobot exploration of Titan and the required autonomy capabilities [4-9]. We describe the aerobot autonomy architecture being developed at JPL, and discuss some of the key component technologies. We also show results from autonomous flight tests conducted in the Mojave Desert.

## SATURN'S MOON, TITAN

Titan is the largest moon of Saturn, with a radius of 2,575 km. It has an atmosphere with a surface density of  $5.55 \text{ kg/m}^3$  (4.6 times the density of Earth's atmosphere at sea level), and an estimated composition of 95% nitrogen, 3% methane, and 2% argon. The surface pressure is approximately 1.5 bar, and the gravity at the surface is  $1.35 \text{ m/s}^2$  (1/7 of the gravity of Earth). The surface temperature is approximately  $-180^\circ \text{ C}$  or

<sup>1</sup> 1-4244-1488-1/08/\$25.00 ©2008 IEEE.

<sup>2</sup> IEEEAC paper #1296, Version 2, updated 2007:11:22.

Author's Current Address:

A. Elfes, J.L. Hall, E.A. Kulczycki, D.S. Clouse, A.C. Morfopoulos, J.F. Montgomery, J.M. Cameron, A. Ansar and R.J. Machuzak Jet Propulsion Laboratory, Pasadena, CA 91109, USA.

Based on a presentation at the 2008 Big Sky Conference.

0885/8985/08/USA \$25.00 © 2008 IEEE

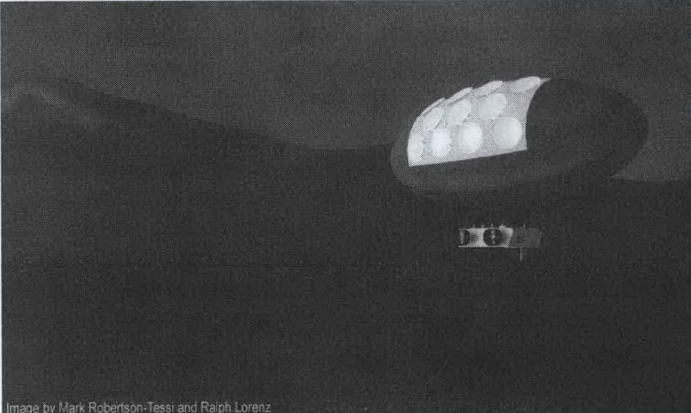
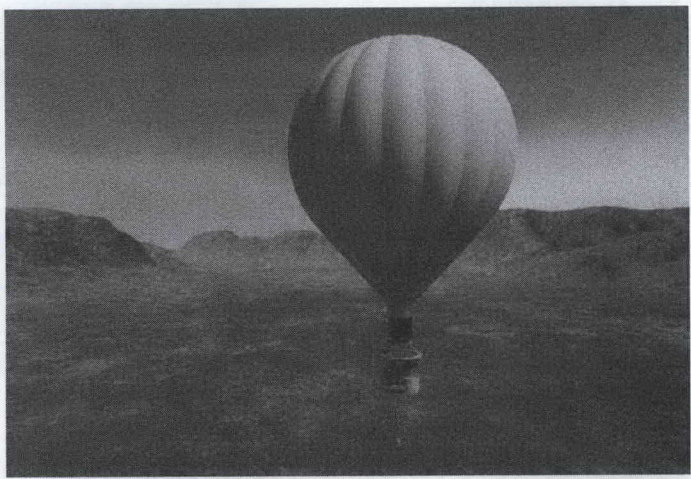
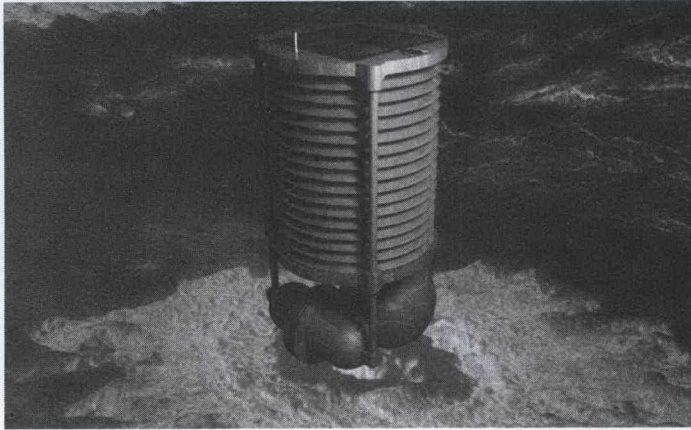
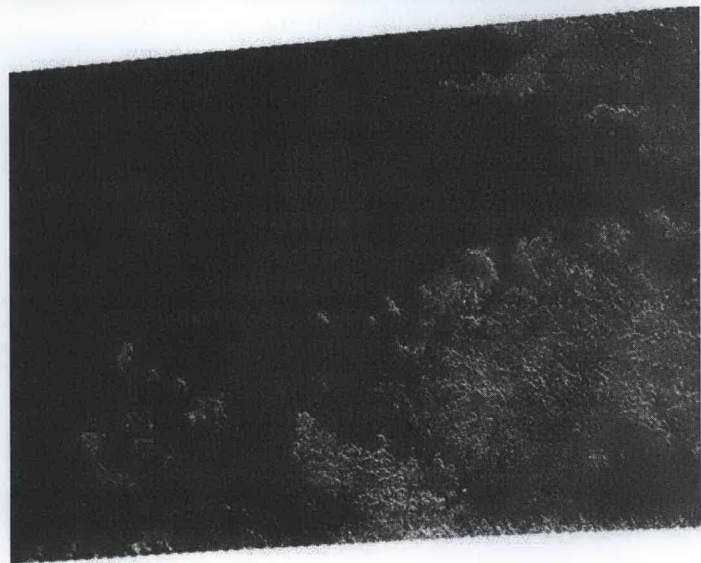
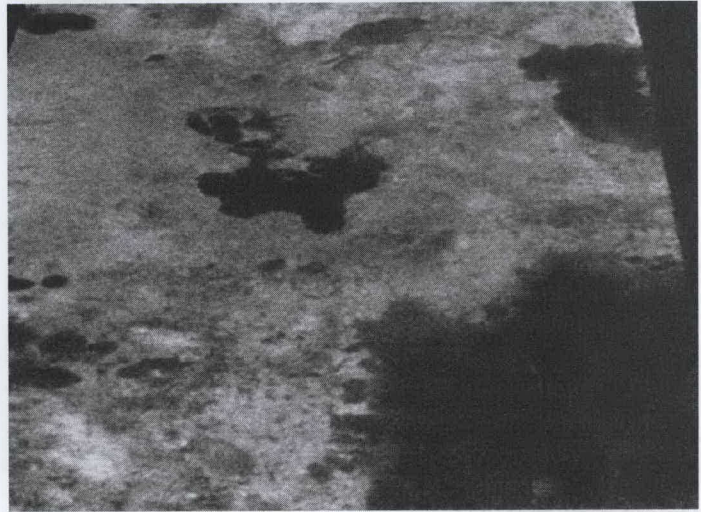
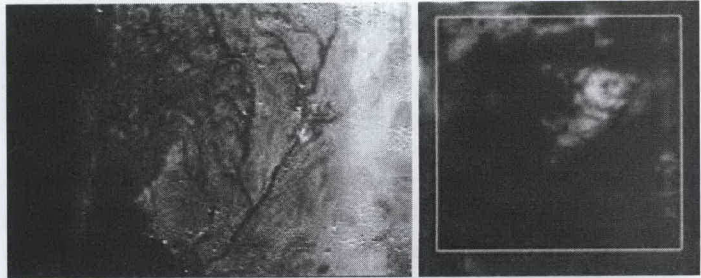


Image by Mark Robertson-Tessi and Ralph Lorenz



**Fig. 1. Lighter-Than-Air Vehicles for Solar System Exploration.** Mission concepts discussed in the 2006 NASA Solar System Exploration Roadmap include a Titan wind-driven Montgolfiere balloon (top), a Titan self-propelled airship (middle), and the Venus Mobile Explorer, an airship with a metal bellows envelope (bottom)

93° K. The upper atmosphere of Titan has a thick haze, caused by sunlight-induced chemical reactions of methane, which shrouds the surface of Titan from visual observation. Early Voyager fly-by observations and recent Hubble Space Telescope (HST) images in the near-infrared spectrum



**Fig. 2. Geological structures identified on Titan.** The upper left image was taken by the visual camera during Huygens descent, showing a river delta topography. The upper right image taken with the Cassini multispectral imager shows a cryovolcano (in light color) that probably brings liquid water and methane to the surface. The middle image taken with the Cassini radar (displayed in false color) shows several large methane lakes in the northern latitudes, and the lower radar image shows the coastline and numerous island groups at the edge of what is presumed to be a large methane sea.  
*Sources: ESA/NASA/JPL/University of Arizona*

indicated the possible existence of continental masses composed of solid rock and frozen water ice, and of liquid bodies potentially composed of liquid ethane and methane [4,5,10]. Additional long-term observations have also provided indications of weather on Titan, including clouds and storms. The successful descent of the Huygens probe to the surface of Titan on January 14, 2005 has provided spectacular images of a very complex terrain, including river channels and drainage basins, sand dunes, and sierras (Figure 2).

Further images and scientific data being obtained from fly-bys by the Cassini spacecraft have unveiled a world with methane lakes, cryovolcanos, and a wide variety of other features (Figure 2).

## AEROBOT AUTONOMY ARCHITECTURE

The main challenges for aerobot exploration of Titan include: large communication latencies, with a round-trip light time of approximately 2.4 hours; extended communication blackout periods with a duration of approximately 8 Earth days, caused by the tidally-locked rotation of Titan in its orbit around Saturn; extended mission duration, currently projected to be on the order of six months to one year; and operation in a substantially unknown environment, with very little data on wind patterns, meteorological conditions, and only low-resolution radar maps of surface topography obtained from Cassini.

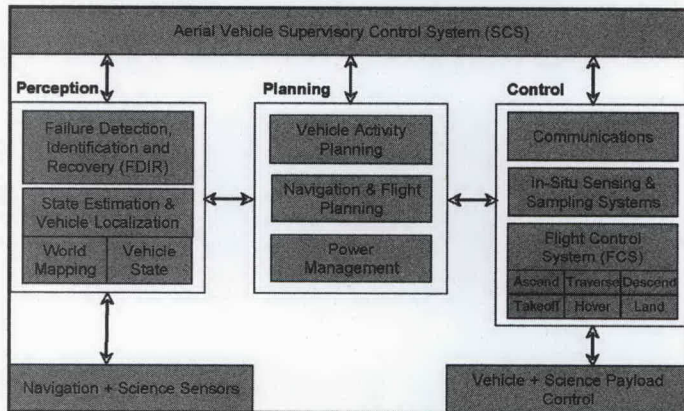


**Fig. 3. Aerobot autonomy architecture with major subsystems**

These challenges lead to several desired capabilities for a Titan aerobot: vehicle safing, so that the integrity of the aerobot can be ensured over the full duration of the mission and during extended communication blackouts; accurate and robust autonomous flight control, including deployment, long traverses, hovering/station-keeping, and touch-and-go surface sampling; spatial mapping and self-localization in the absence of a global positioning system on Titan; and advanced perceptual hazard and target recognition, tracking, and visual servoing, allowing the aerobot to detect and avoid atmospheric and topographic hazards, and also to identify,

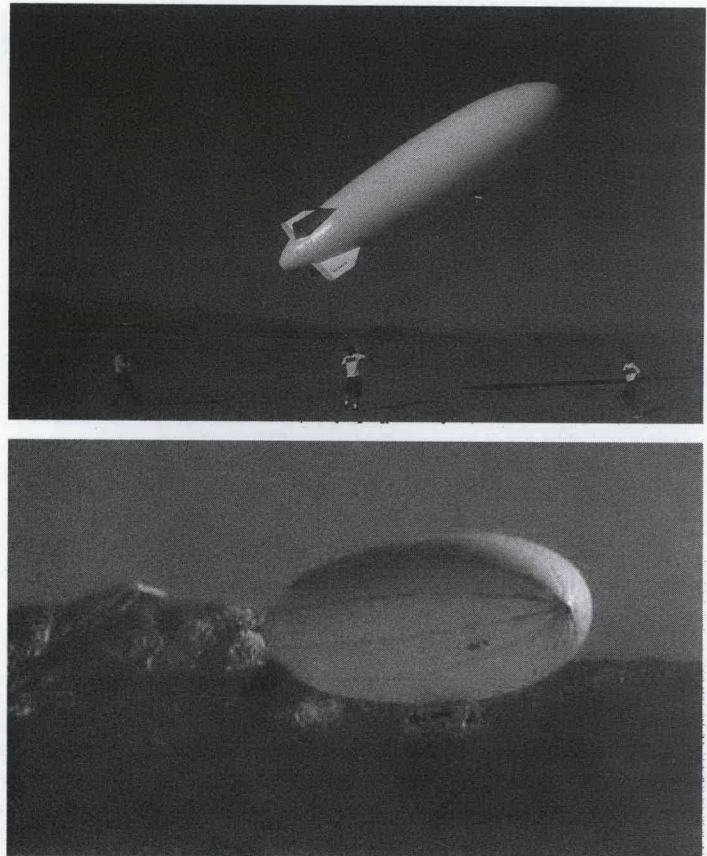


**Fig. 4. The JPL aerobot during autonomous flight tests.**  
These flight tests were conducted at the El Mirage dry lake in the Mojave Desert. The upper image shows liftoff, and the bottom image shows the airship in autonomous flight mode

home-in, and keep station over pre-defined science targets or terrain features. It should be noted, however, that a variety of mission scenarios can be implemented with a subset of these autonomy capabilities [5, 6].

In preparation for a future Titan mission, we are developing an aerobot autonomy architecture that integrates accurate and robust vehicle and flight trajectory control, perception-based state estimation, hazard detection and avoidance, vehicle health monitoring and reflexive safing actions, multi-modal vehicle localization and mapping, autonomous science, and long-range mission planning and monitoring (Figure 3).

Lower level functions in the autonomy architecture include sensor and actuator control, vehicle state estimation, flight mode control, supervisory flight control, and flight profile execution. Intermediate level functions include vehicle health monitoring, failure detection, identification and recovery (FDIR), flight trajectory and profile planning, and image-based navigation. The latter provides GPS-independent localization, as well as local and regional mapping. Higher-level functions include mission planning, resource management, and mission execution and monitoring.

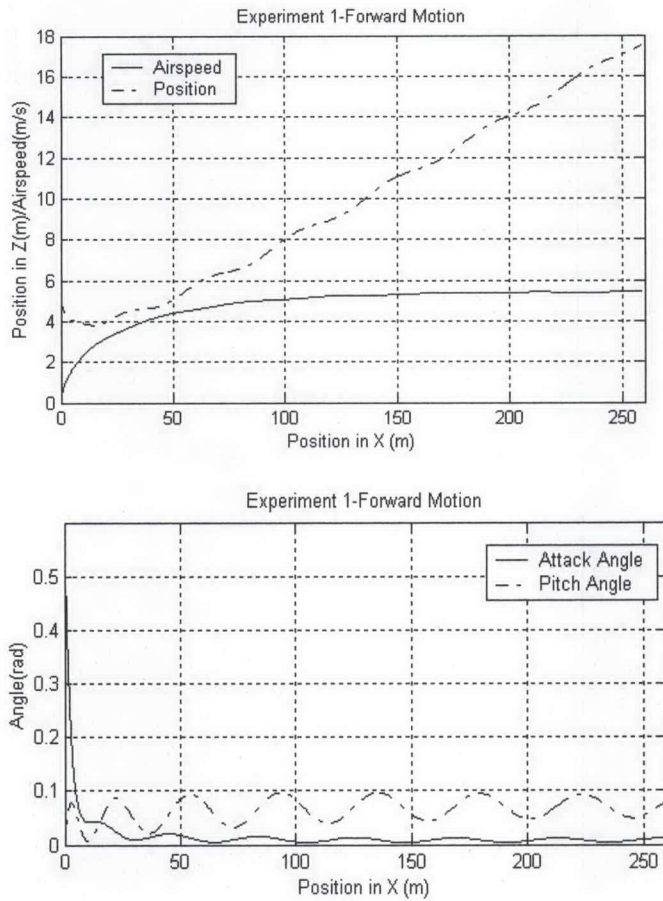


**Fig. 5. Aerodynamic model simulation: forward motion. The forward motion and the corresponding attack and pitch angles are shown. The z axis points up**

Herein, we concentrate on the flight control, vehicle simulation, and on-board navigation systems. This includes development of a robust flight control system based on vehicle aerodynamic modeling, system simulation for robust control law development and testing, and vehicle system identification; and accurate vehicle multi-sensor state estimation methods, using both inertial and vision-based motion and position estimation.

### THE JPL AEROBOT TESTBED

The current prototype JPL aerobot testbed (Figure 4) is based on an Airspeed Airship AS-800B [11]. The airship specifications are: length 11 m, diameter 2.5 m, total volume 34 m<sup>3</sup>, two 2.3 kW (3 hp) 23 cm<sup>3</sup> (1.4 cu inch) fuel engines, double catenary gondola suspension, control surfaces in an "X" configuration, maximum speed of 13 m/s (25 kts), maximum ceiling 1000 m, average mission endurance 60 minutes, static lift payload 12 kg ASL, and dynamic lift payload up to 16 kg ASL. The avionics and communication systems are installed in the gondola.

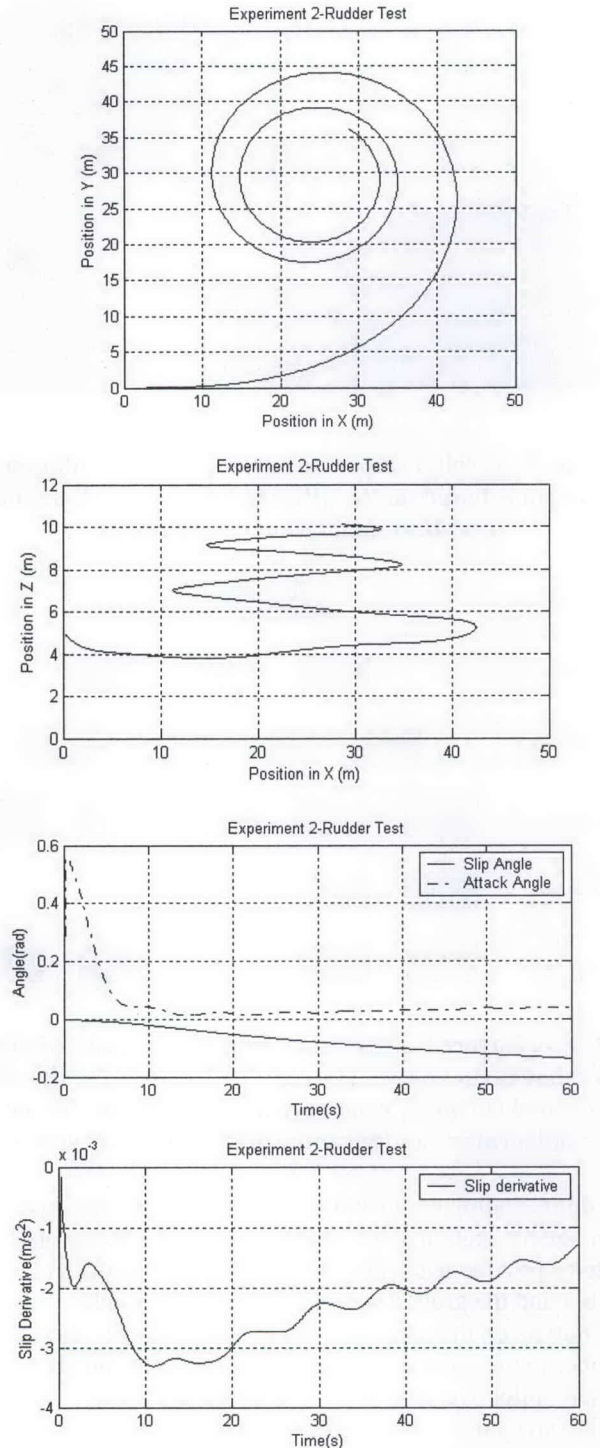


**Fig. 6. Aerodynamic model simulation: rudder deflection. The plots show control surface deflection equivalent to rudder actuation, resulting in a limit cycle flight trajectory. The z axis points up**

The aerobot avionics system is built around a PC-104+ computer architecture. The processor stack has a serial board interface to the navigation sensors, a PWM board for reading pulsedwidth modulated signals from the human safety pilot and generating PWM signals based upon control surface commands from the avionics software, and an IEEE 1394

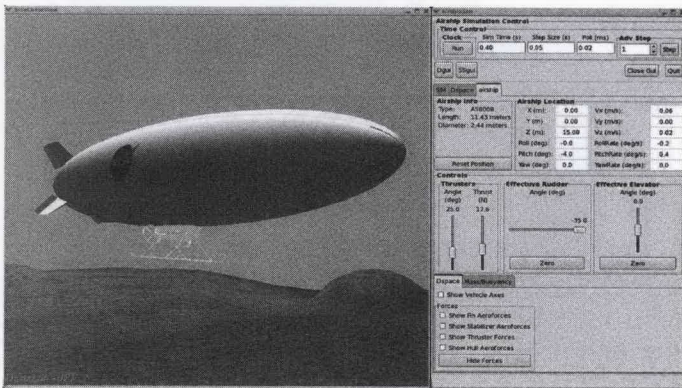


**Fig. 7. Aerobot simulation system. The simulation system is based on the JPL DARTS/Dshell dynamic real-time simulation environment**

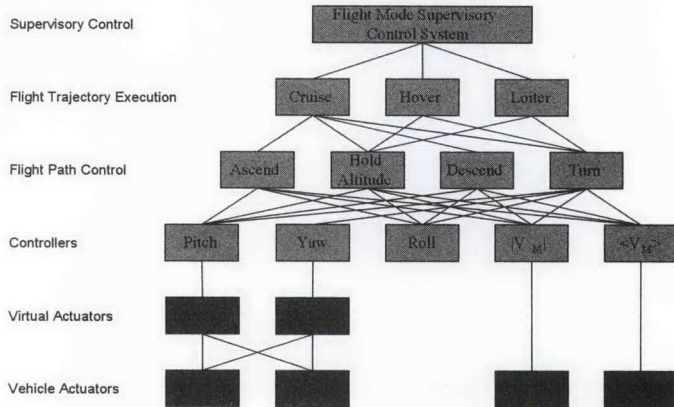


**Fig. 8. Layered supervisory control structure of the aerobot flight control system. "CS" stands for the tail control surfaces, which are arranged in an "X" or ruddervator configuration. VM is the trust vector**

board for sending commands to, and reading image data from, the navigation and science cameras. Wireless serial modems provide data/control telemetry links between the aerobot and the ground station, and additional video transmitters on the aerobot provide downlinks of video imagery to the ground station. The safety pilot can always reassert "pilot override" control over the aerobot.

The navigation sensors currently consist of an IMU (angular rates, linear accelerations), a compass and inclinometer (yaw, roll, and pitch angles), and a DGPS (for absolute 3-D position). The vision sensors include two down-looking navigation cameras, one with a  $360^\circ \times 180^\circ$  field of view and another with a narrower FOV. Additionally, we have a laser altimeter (surface relative altitude), a barometric altimeter (absolute altitude ASL), and an ultrasonic anemometer (for relative wind field measurements).

The ground station is composed of a laptop, a graphical user interface to the vehicle, wireless data and video links,

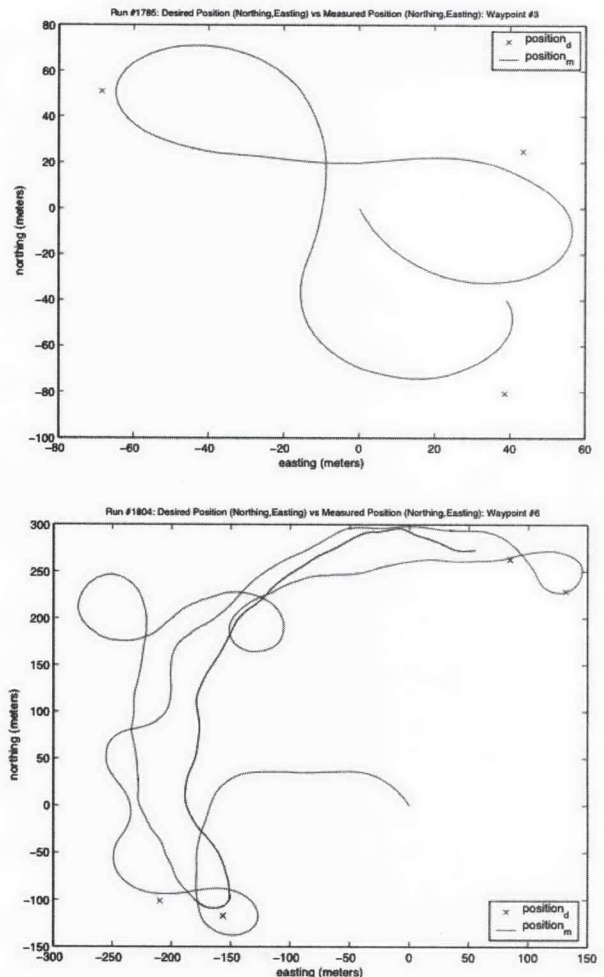


**Fig. 9. Waypoint flight control. Top: three waypoints have been reached, with an operator-defined threshold of 25 m to the GPS coordinates of the target. Bottom: Waypoint flight control under severe wind disturbances. All waypoints were reached. A trajectory in red indicates that the vehicle is flying autonomously, while green indicates that the aerobot is under pilot control**

video monitors and VCRs, and a differential GPS (DGPS) base station that provides 3-D vehicle position estimates with an accuracy on the order of centimeters. Field tests of the JPL aerobot are conducted at the El Mirage dry lake site in the Mojave Desert (Figure 4).

It should be noted that our testbed is not meant to be a high fidelity prototype of a Titan blimp, but rather a convenient platform for autonomy technology development.

## AEROBOT AERODYNAMIC MODELING

The aerobot flight control system being developed is based on: 1) system modeling, which includes aerodynamic, airship sensor and actuator, and environmental modeling; 2) system identification for aerodynamic parameter estimation; 3) model and control system validation in a

physically-based simulation environment; and 4) flight testing on the aerobot testbed.

The aerodynamic model developed for the JPL airship is significantly different from fixed-wing or rotary-wing aircraft aerodynamic models, as the virtual mass and inertia properties of the displaced atmospheric volume are substantial when compared with those associated with the vehicle itself. Additionally, an aerobot is characterized by having different flight modes (take-off/landing, station-keeping/hovering, loitering, ascent/descent, high-speed cruise, low-speed flight) that require alternative actuator control strategies and flight control algorithms. Important airship flight control challenges include non-minimum phase behavior and oscillatory modes at low speeds, time-varying behavior due to altitude variations, and variable efficiency of the actuators depending on aerobot speed [12,13].

We developed a new non-linear robotic airship model intended for control system design and evaluation. The model brings together much of the previous airship modeling results available in the literature, and adds new elements to extend the model's range of applicability. In addition, it is built from a systems-design-control interaction perspective, in which physical elements are parameterized to easily make design changes as control systems are designed and evaluated. The kinematic and dynamic equations of the model are based in part on [14], and are not repeated herein due to space constraints.

The aerodynamic model developed has the ability to characterize all four primary modes of flight (launch, cruise, hover, landing). In order to make the model as versatile as possible for changing flight conditions and optimization studies, all airship dimensions are given parametric definitions. The reference frame for the airship is the hull center of volume and is defined using a North-East-Down orientation, as is typically done with aircraft.

Initial validation of the model was done running various simulations and assessing the vehicle. We summarize below some of the results: a complete description of the model; a more extensive set of validation experiments; and the corresponding results are found in [14].

### Forward Motion

Both thrusters were given a step input of 4 N with zero angle relative to the airship; the fins had zero deflection. The airship had  $V_0 = 0$  and started at an elevation of 5 m. As expected, the airship initially pitches upward as it loses altitude (Figure 5). The pitch upward is due to the step input to the engines whereas the heaviness condition (negative buoyancy) of the vehicle causes the drop in elevation. As the airship gains speed, the pitch angle begins oscillating about a positive value, creating aerodynamic lift as verified under field conditions.

### Rudder Test

Control surface behavior was tested by inputting a  $-20^\circ$  deflection angle and repeating the previous test. The angle

represents the deflection of the upper port and upper starboard fins about their center axis. As previously described, the opposing fins are rigidly coupled. This results in a negative slip angle that moves the airship to port. The trajectory in the XY plane gradually converges to a circle (Figure 6, top). This is also shown in Figure 6 (bottom), where the slip angle derivative approaches zero. In the XZ plane (Figure 6, center), the airship gains altitude due to the upward pitch, as discussed previously.

## SIMULATION SYSTEM

The aerobot aerodynamic model developed has been implemented both in Matlab, C, and using the DARTS/Dshell dynamics and real-time simulation system developed at JPL [15]. The former is being used for control system development, while the latter has been used to build a highly flexible simulation platform for aerobot missions. The aerobot DARTS/Dshell simulator uses high-fidelity physics model for aerodynamics, mass properties, buoyancy, kinematics, dynamics, control surfaces, etc., and can also incorporate simulated sensor and a wide variety of terrain models. The aerodynamic model developed in C is integrated with the aerobot flight software and is currently being used for pre-flight controller validation. In the future, this integrated model will allow for the use of Model Predictive Control Methods on the JPL Aerobot. The models are parameterized, so that the simulation can be used to represent many types of airships. The initial implementation is based on parameters for the JPL aerobot. We have also developed a GUI to operate the airship controls and monitor the airship response (Figure 7). Simulations can be run with or without the GUI. The modeling and implementation work has been largely completed, while the model and simulation validation has been started. A variety of system identification tests will be run using the actual JPL aerobot to obtain accurate estimates for a number of model parameters. Once this is done, the simulation platform can also be used to test control software.

## AUTONOMOUS FLIGHT CONTROL

The autonomous flight system has a layered supervisory control structure (Figure 8). It oversees the main flight trajectory modes (cruise, hover, and loiter), which use ascent, descent, turn, and altitude controllers. These, in turn, command the vehicle attitude and thrust controllers. For an "X-tail" configuration, the opposing tail surfaces (1+3 and 2+4) are operated in a coupled mode. This means there is no direct roll control, and also that "pure" elevator and rudder behavior is implemented through actuation of all four control surfaces.

The first version of the on-board flight autonomy system has been implemented using PI controllers for pitch, yaw, and altitude control, and corresponds to the "controller" and "flight path control" levels in the supervisory control architecture (Figure 8). We recently added PI controllers for

throttle and currently are developing robust lead-lag controllers for pitch, yaw, and altitude control based on aerodynamic models, which will allow us to do accurate 3-D trajectory execution. Throttle and thrust vector controllers for hovering operations are currently under development to be scheduled in at low airspeeds. We have also initiated work on using the full aerodynamic model and the associated simulation tools to develop a next generation set of robust controllers, which we expect will demonstrate tighter vehicle control and more accurate trajectory control under wind disturbances.

### Waypoint Flight Control

At the flight trajectory execution control level in the supervisory control architecture (Figure 8), we have implemented a waypoint flight control system. Waypoints are specified by the operator, who also sets the satisfying conditions that define when a waypoint has been considered reached. The approach used is called “orienteering,” where the control objective is defined in terms of reaching the waypoint, rather than in terms of the deviation from a given trajectory.

Figure 9 shows autonomous waypoint flight control tests, again conducted at El Mirage. Figure 9 (top) shows waypoint flight control for a sequence of 3 waypoints. A waypoint is specified as having been reached if the aerobot is within a Euclidean distance of 25 m from the GPS waypoint coordinates. Atmospheric conditions were moderate, with wind speeds below 5 knots. Figure 9 (bottom) shows an autonomous flight test under substantial wind conditions, with gusts up to 10 knots. The airship is blown off the direct waypoint route on several occasions when it is in a beam reach (orthogonal) condition relative to the wind direction. Additionally, it is occasionally yawed off course when heading into or crossing the wind. Nevertheless, the autonomous flight control system was able, even under these severe wind disturbances, to visit all waypoints. We plan to address wind disturbances explicitly through the incorporation of an  $H_m$  robust controller design [12].

### IMAGE-BASED MOTION ESTIMATION

Pose (position and orientation in 6 DOF) and motion estimation is currently done by the fusion of IMU and GPS data using a Kalman filter, allowing assessment of the vehicle flight control and trajectory following accuracy. To achieve global and regional localization on Titan in a GPS-independent manner, we are investigating both celestial trackers for ephemerides-based global position estimates, and developing an image-based motion estimation (IBME) system with an associated multi-sensor state estimation filter that is used to fuse inertial and visual navigation estimates [16]. At this point, only imagery from the down-looking camera is used (Figure 10).

Initial results have been very encouraging. The IBME system developed gives us estimates of the pose and motion



**Fig. 10. Science and navigation cameras.** The upper image is from the forward-looking science camera, while the lower image is from the down-looking navigation camera

of the aerobot (Figure 11, top), performs image mosaicking for visual mapping purposes (Figure 11, bottom), and also recovers 3-D terrain structure information.

An important open issue is the use and performance of an IBME system in support of vehicle localization under the actual lighting conditions on Titan. Estimates of day-time lighting conditions indicate that flight-qualified visual spectrum cameras would be adequate for IBME. We are currently investigating what conditions will be encountered for night-time navigation, and whether cameras operating in infrared spectral bands would be required.

Another open issue is the impact of image texture on IBME performance. Images with few distinctive landmark features or patterns degrade IBME performance, a problem that is also directly related to camera resolution and sensitivity, as well as to the observation altitude of the

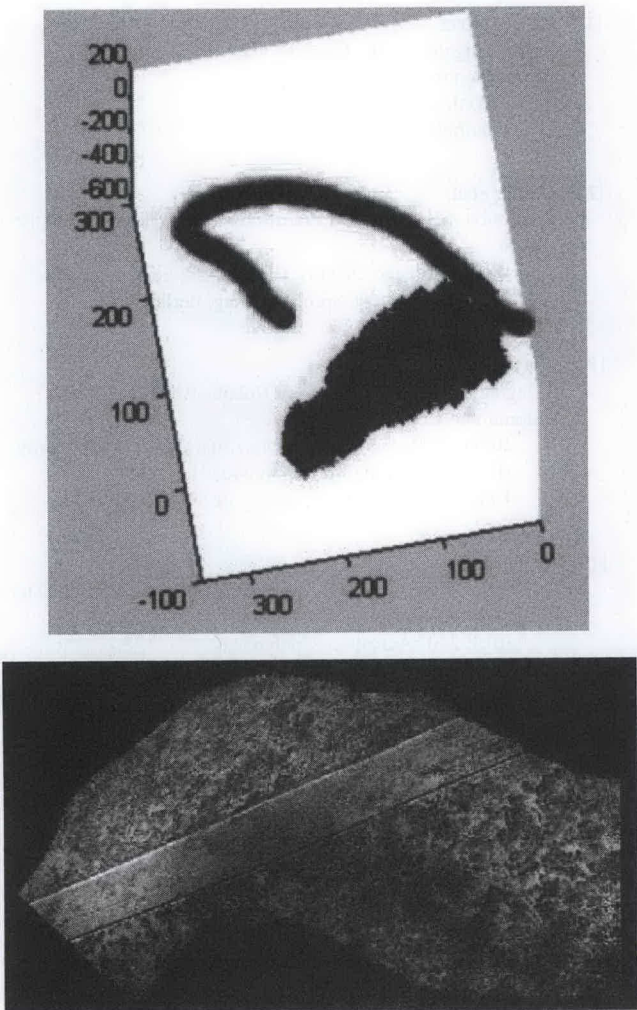


**Fig. 11. Image-based motion estimation (IBME).** Image sequences obtained from the down-looking navigation camera are registered to each other, allowing aerobot trajectory estimation (top, in green) and image mosaicking for regional visual mapping generation (bottom). Scaling is obtained using altitude estimates from other sensors, such as barometric or laser altimeters. The blue patch (top) indicates matched areas of multiples images; units are in meters

aerobot. Titan sand dunes fields seem to display repetitive patterns, while hills and coastal areas have significant texture, and methane lake surfaces seem to be largely featureless (except in some of the shallows, where the bottom may be visible). We plan to conduct further investigations into IBME performance for different surface texture conditions.

## CONCLUSIONS

LTA systems are a strategic platform for the exploration of planets and moons with an atmosphere such as Venus, Mars, and Titan. Aerobots, in particular, can provide geographically extensive science data at high resolutions and over varied terrains to a degree that cannot be matched by

surface-bound rovers or other aerial vehicles. At the same time, operation of an aerobot at Titan or other destination in the solar system imposes significant long-term autonomy requirements.

We outlined above an architecture for a substantially autonomous aerobot, described the current JPL aerobot testbed, and discussed initial steps toward the development of an aerobot flight control and navigation system.

Our next steps include performing robust system identification, improving the flight control system robustness and accuracy, developing a trajectory following system for systematic surveys, and integrating vision-based localization and navigation capabilities.

## ACKNOWLEDGMENTS

The research described herein was performed at the Jet Propulsion Laboratory, California Institute of Technology, under a contract with the National Aeronautics and Space Administration (NASA), with initial funding from the Intelligent Systems (IS) Program (SMD) and current funding from the Research and Technology Development (RTD) program at JPL. The views and conclusions contained herein are those of the authors and should not be interpreted as representing the official policies, either expressed or implied, of the sponsoring organizations.

## REFERENCES

- [1] Solar System Exploration. Technical Report, NASA, Washington, DC, 2003.
- [2] NASA. 2006 Solar System Exploration Strategic Roadmap, Technical Report, NASA, Washington, DC, 2006.
- [3] J. Cutts, P. Beauchamp, A. Elfes, J.L. Hall, T. Johnson, J. Jones, V. Kerzhanovich, A. Yavrouian and W. Zimmerman. Scientific Ballooning at the Planets. In Proceedings of the 2004 COSPAR Conference. Paris, France, July 2004.
- [4] J.L. Hall, V.V. Kerzhanovich, J.A. Jones, J.A. Cutts, A.A. Yavrouian, A. Colozza and R.D. Lorenz. Titan Airship Explorer, in Proceedings of the 2002 IEEE Aerospace Conference, IEEE, Big Sky, Montana, March 2002.
- [5] J.L. Hall, A. Elfes, T. Spilker, V. Kerzhanovich and J.F. Montgomery. Titan Aerobots: An Overview of Mission Scenarios and Required Autonomy Technologies. Whitepaper, JPL 2002.
- [6] J.L. Hall, V.V. Kerzhanovich, A.H. Yavrouian, J.A. Jones, C.V. White, B.A. Dudik, G.A. Plett, J. Mennella and A. Elfes (2004). An Aerobot For Global In Situ Exploration of Titan, 35<sup>th</sup> COSPAR Scientific Assembly, Paris, France, July 20-24, 2004.

- [7] A. Elfes, J.L. Hall, J.F. Montgomery, C.F. Bergh and B.A. Dudik,  
Towards a Substantially Autonomous Aerobot for Exploration  
of Titan.  
In Proceedings of the International Conference on Robotics  
and Automation (ICRA 2004),  
IEEE, Las Vegas, Nevada, May 2004.
- [8] A. Elfes et al.  
Robotic Airships for Exploration of Planetary Bodies with an  
Atmosphere: Autonomy Challenges.  
Journal of Autonomous Robots,  
Vol. 14, No. 2/3.  
Kluwer Academic Publishers, The Netherlands, 2003.
- [9] A. Elfes, J. Hall, E. Kulczycki, A. Morfopoulos, J. Montgomery,  
D. Clouse, D. Bayard, J. Cameron, R. Machuzak, L. Magnone,  
C. Bergh and G. Walsh.  
Autonomy Capability Development for a Titan Aerobot.  
Fourth Annual International Planetary Probe Workshop  
(IPPW-4), Pasadena, CA, June 2006.
- [10] R.D. Lorenz.  
Post-Cassini Exploration of Titan: Science Rationale and Mission  
Concepts.  
In Journal of the British Interplanetary Society,  
Vol. 53, UK, 2000.
- [11] N. Foster.  
Airspeed Airships.  
<http://www.airspeedairships.com>, 2003.
- [12] S.B.V. Gomes.  
An Investigation of the Flight Dynamics of Airships with  
Application to the YEZ-2A.  
PhD thesis, College of Aeronautics,  
Cranfield University, 1990.
- [13] A. Elfes et al.  
Perception, Modelling and Control for an Autonomous Robotic  
Airship.  
In H.I. Christensen, G.D. Hager (eds.), Sensor Based  
Intelligent Robots, SpringerVerlag, Berlin, 2001.
- [14] J. Payne and S.S. Joshi.  
6 Degree-of-Freedom NonLinear Robotic Airship Model for  
Autonomous Control.  
Robotics, Autonomous Systems, and Controls Laboratory  
(RASCAL) Technical Report 040521,  
University of California, Davis, 21 May 2004.
- [15] J. Balaram et al.  
DSENDs - A High-Fidelity Dynamics and Spacecraft Simulator for  
Entry, Descent and Surface Landing,  
IEEE 2002 Aerospace Conference,  
Big Sky, Montana, March 2002.
- [16] S.I. Roumeliotis, A.E. Johnson and J.F. Montgomery.  
Augmenting Inertial Navigation with Image-Based Motion  
Estimation.  
In Proceedings of the 2002 IEEE International Conference  
on Robotics and Automation, Washington, DC, 2002.